Increase in canopy turnover during El Niño drought conditions in Amazon forests from multi-temporal airborne lidar

Veronika Leitold [1]
Douglas C Morton [1]
Michael Keller [2,3]
Maiza Nara dos-Santos [3]
Marcos Longo [3]
Marcos Scaranello [3]

[1] NASA Goddard Space Flight Center (GSFC)
8800 Greenbelt Road - Greenbelt, MD - 20771 - USA
{veronika.leitold, douglas.morton}@nasa.gov

[2] NASA Jet Propulsion Laboratory (JPL)
4800 Oak Grove Drive - Pasadena, CA - 91109 - USA
mkeller.co2@gmail.com

[3] EMBRAPA Informática Agropecuária
Caixa Postal: 6041 - 13083-886 - Campinas - SP, Brasil
{maizanara, mdplongo, masscaranello}@gmail.com

Abstract. Amazon forests store large amounts of carbon in biomass and have a strong influence on the terrestrial carbon sink. Under growing human pressure and changing climatic conditions, these ecosystems are at the risk of turning from carbon sink to carbon source. Carbon cycling in intact Amazon forests is driven by the rate of tree mortality; canopy turnover size and frequency can be assessed using remote sensing data, yet the spatial and temporal variability of turnover across the landscape is unclear. We used multi-temporal airborne lidar data from intact and fragmented forest sites in the Tapajós National Forest region in Brazil to estimate spatial and temporal patterns of forest dynamics between 2013-14 and 2014-16. Annualized canopy turnover rates within intact forests increased from a mean of 1.81% yr^{-1} (range 1.68 - 1.95% yr^{-1}) in the first interval to 2.85% yr^{-1} (range 2.51 - 3.13% yr^{-1}) in the second interval. Similarly, annualized turnover values in fragmented forests increased from a mean of 1.98% yr^{-1} (range 1.36 - 3.06% yr^{-1}) in the first interval to 3.12% yr^{-1} (range 2.17 - 4.70% yr^{-1}) in the second interval. The number of turnover events per unit area increased over time in both forest types, but the average size of canopy changes remained largely constant. These findings suggest that El Niño drought conditions may accelerate canopy turnover in all Amazon forests, highlighting the need for multi-temporal lidar over large areas to further constrain the Amazon carbon budget.

Keywords: airborne lidar, tropical forest dynamics, disturbance and degradation, carbon cycle, lidar aéreo, dinâmica de florestas tropicais, perturbação e degradação, ciclo do carbono.

1. Introduction

Tropical rainforests play an important role in the global carbon cycle by absorbing CO_2 from the atmosphere and storing it in biomass (Le Quéré et al., 2016). The Amazon is the largest remaining intact tropical forest in the world, and Amazon forests therefore have a strong influence on the magnitude and variability in the terrestrial carbon sink (Brienen et al., 2015; Gatti et al., 2014). The net carbon balance of the Amazon also reflects emissions from growing human pressure in the form of deforestation, degradation and fragmentation (van der Werf et al., 2010). Additionally, natural disturbances induced by severe droughts and widespread forest fires in recent years have also adversely affected the natural cycling of carbon in these ecosystems, turning them from a net carbon sink into a net carbon source (Feldpausch et al., 2016). Large uncertainties remain regarding the magnitude of carbon fluxes in tropical forests and the spatial distribution of carbon stocks across the landscape (Pan et al., 2011).

To improve our estimates of current and future carbon cycling in Amazon forests, we need to better understand the processes of disturbance and recovery, including the size and frequency of turnover events (Lloyd et al., 2009). Field inventory plots can track and measure tree mortality with great precision (Feldpausch et al., 2016; Brienen et al., 2015; Phillips et al. 2009), but they are limited in spatial extent and may not capture landscape-scale processes. At the other extreme, satellite observations can capture and monitor large regions of the land surface (Chambers et al., 2013; Hansen et al., 2013), but don't provide sufficient spatial detail to account for small-scale changes in the forest canopy. Airborne lidar has been used to bridge the gap between field-based measurements and satellite observations by providing detailed, three-dimensional information on forest structure (Espírito-Santo et al., 2014; Asner et al., 2013). Repeat lidar measurements of the same forest areas enable us to identify changes in the forest canopy over time (Marvin and Asner, 2016; Hunter et al., 2015), leading to a better understanding of the processes of turnover dynamics and better estimates of the associated carbon fluxes.

In this study, we analyzed a series of high-density, small-footprint airborne lidar data from intact and fragmented forest sites in the Tapajós National Forest (TNF) region in the Brazilian Amazon. We compared the structure and dynamics of an intact forest area within the TNF with remaining fragments of forest in the surrounding landscape that were not logged or burned during the study period. We identified canopy turnover events over two consecutive time periods, 2013-14 and 2014-16, and compared the estimated rates of turnover across forest types during these intervals. The region was subjected to intense El Niño drought conditions in 2015-2016, and any drought-related changes in canopy structure are included in the second lidar sampling interval. Our study specifically addressed the following four questions: (1) How do canopy turnover rates differ between intact and fragmented forests? (2) Do turnover rates in intact and fragmented forests change over time? (3) What fraction of the estimated turnover is due to branch-fall, tree-fall or multiple tree-fall events? (4) Is the size distribution of turnover events similar or different in intact versus fragmented forests?

2. Methods

2.1. Data collection

Our study site is located in the Brazilian Amazon near the city of Santarém, PA (Figure 1). Airborne lidar data were collected along two 50 km transects (200m width, 995 ha area) at three different times: September 2013 (t1), June 2014 (t2), and March 2016 (t3). The time intervals between lidar collections were 0.75yrs (t1-t2) and 1.83yrs (t2-t3). The first transect, ST1, covers a section of intact old-growth *terra firme* forest within the Tapajós National Forest (TNF). The ST2 transect parallels the ST1 transect on the opposite side of the BR-163 highway and covers a range of different land cover types. Lidar data were collected with very high return density: 9.2 - 10.8 ppm^2 in 2013, 39.6 - 59.9 ppm^2 in 2014, and 29.3 - 33.9 ppm^2 in 2016. The first two surveys used an Optech ALTM Orion laser scanner at 853m average flight altitude, 11º field of view, and 65% flight line overlap. The third survey used an Optech ALTM 3100 laser scanner at 650m average flight altitude, 15º field of view, and 70% flight line overlap. The original lidar data used in this study, as well as the metadata information, are freely available from the Sustainable Landscapes Brazil Project's webgis at https://www.-paisagenslidar.cnptia.embrapa.br/webgis/.

ISBN: 978-85-17-00088-1

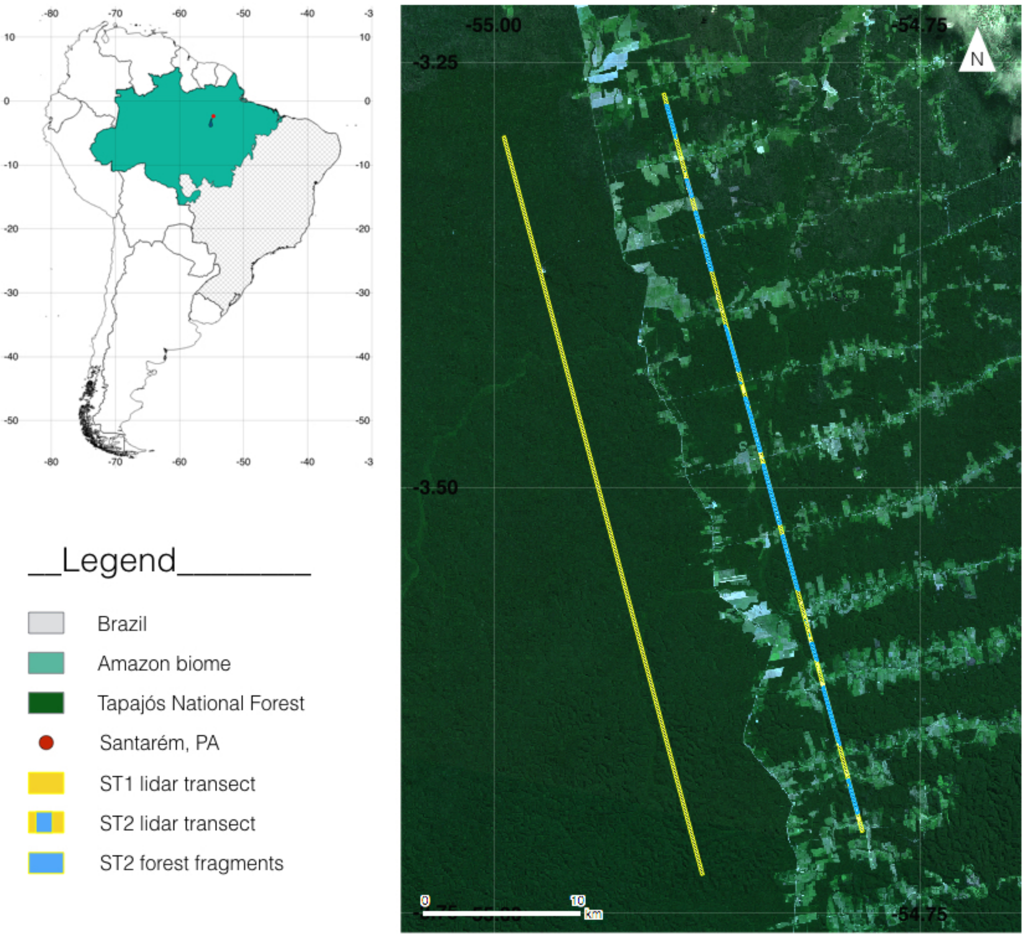

Figure 1. Map of the study area showing the location and extent of the two lidar transects: ST1 (intact forest) and ST2 (forest fragments and other land cover types).

2.2. Data processing and analysis

Lidar return data from the three collections (t1, t2, t3) were merged to generate a single digital terrain model (DTM) in order to normalize height estimates from t1, t2 and t3 data. Canopy height models (CHMs) at 0.5m spatial resolution were then generated separately for t1, t2 and t3 following standard lidar processing methods (Cook et al., 2013). Canopy turnover events were identified based on contiguous clusters (≥ 4m^2) with large changes in canopy height (≥ 3m) between lidar collections (Figure 2).

For the analysis of intact forest structure and changes, the ST1 transect was divided into five subsections (ST1a, b, c, d and e) of 205 ha each, with ST1e being slightly smaller (167 ha). On the opposite side of the highway, land cover types within the ST2 transect were evaluated using visual assessment of a contemporary Landsat 8 surface reflectance imagery (Path 227 Row 062, Date 2016-June-30, Source: USGS) as well as lidar return distributions and canopy height information derived directly from the lidar data. We identified 12 different fragments of remaining contiguous forest area where canopy cover was ≥ 10%, mean canopy height was ≥ 20m, and the width of the forest patch was ≥ 20m (see Figure 1). The area of the resulting fragments (labeled FR01 through FR12) ranged from 23.5 ha to 80.0 ha.

ISBN: 978-85-17-00088-1

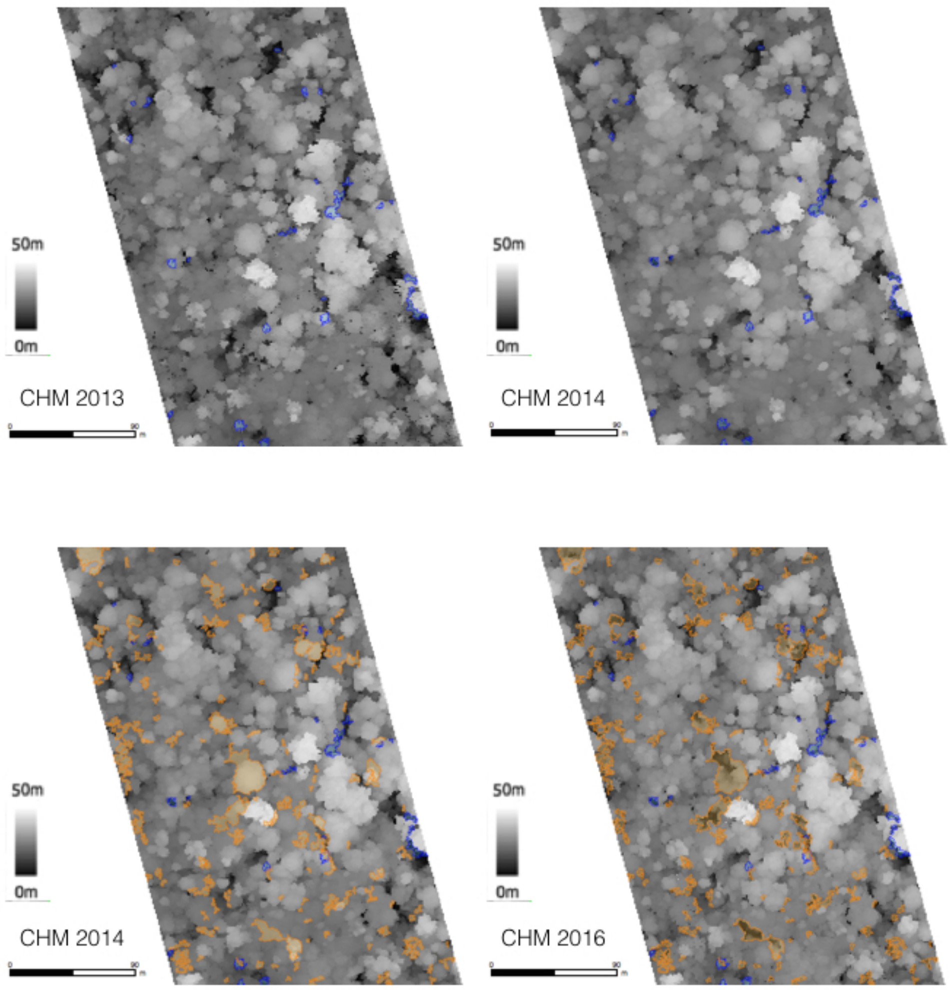

Figure 2. Canopy height models from the three lidar collections (2013, 2014, 2016) and the canopy turnover events identified between 2013-2014 (in blue) and 2014-2016 (in orange).

3. Results and Discussion

3.1. Forest characteristics

Parallel transects in this study captured similar variability in terrain elevation and forest characteristics inside and outside the TNF (Table 1). Terrain elevation varied between 50-250 m a.s.l. and slope followed a north-south gradient, with more steeply sloped terrain in the southern sections (13.4º mean slope, STd-e and FR09-12) than northern portions of the transects (5.2º mean slope, STa-c and FR01-08). The distribution of canopy heights along ST1 was consistent among segments with little variation in mean canopy height values (average 27.8m; range from 25.7m to 29.3m). The forest canopy in the ST2 fragments was generally shorter than in the intact ST1, with mean canopy height values ranging between 21.8m (FR05) and 26.6m (FR01), and with an average value of 24.5m across all fragments. The intact ST1 segments as well as most forest fragments in ST2 were characterized by left-skewed canopy height distributions (i.e. more taller trees than short ones), while four of the ST2 fragments were right-skewed (FR01, 05, 06 and 12) with more shorter trees than tall ones. Such a shift in canopy heights towards a strongly right-skewed distribution might indicate a history of disturbance in those forest fragments (Longo et al., 2016).

Table 1. Canopy structure and turnover statistics in intact (ST1) and fragmented (ST2) forests.

Transect	Segment/ fragment	Area	Elevation min-max	Terrain slope $\mu \pm \sigma$	Canopy height (t3) $\mu \pm \sigma$	CH Skewness	Turnover t1-t2	Turnover t2-t3	% Δ Turnover
		ha	m	º	m		% yr^{-1}	% yr^{-1}	%
ST1	ST1a	205.5	102 - 209	4.7 ± 4.4	29.3 ± 10.4	-0.389	1.95	2.96	51.8
	ST1b	206.0	60 - 148	5.3 ± 4.8	25.8 ± 8.7	-0.111	1.73	3.13	80.9
	ST1c	206.0	91 - 192	5.5 ± 4.9	28.1 ± 9.0	-0.218	1.68	2.89	72.0
	ST1d	206.0	80 - 209	13.8 ± 10.1	27.1 ± 8.3	-0.117	1.80	2.77	53.9
	ST1e	167.0	99 - 257	17.9 ± 7.9	28.8 ± 9.2	-0.155	1.87	2.51	34.2
ST2	FR01	42.7	76 - 139	7.6 ± 6.4	26.6 ± 8.1	0.074	1.58	3.46	119.2
	FR02	24.3	84 - 161	11.0 ± 7.1	24.9 ± 7.2	-0.183	1.65	3.98	141.2
	FR03	29.7	112 - 136	2.9 ± 1.6	23.8 ± 7.7	-0.211	1.68	3.30	96.8
	FR04	42.1	102 - 144	3.8 ± 2.4	24.9 ± 8.6	-0.328	1.90	3.35	76.3
	FR05	58.4	66 - 151	5.5 ± 6.5	21.8 ± 9.2	0.534	2.46	4.70	91.1
	FR06	26.6	88 - 148	4.5 ± 2.7	23.1 ± 8.6	0.289	2.45	3.66	49.4
	FR07	42.8	57 - 107	5.3 ± 6.4	24.0 ± 7.4	-0.082	1.36	2.07	52.3
	FR08	80.0	59 - 115	6.6 ± 6.5	24.0 ± 8.0	-0.274	1.62	2.73	68.2
	FR09	73.5	71 - 140	11.0 ± 10.0	25.0 ± 7.8	-0.513	2.07	2.17	4.9
	FR10	23.5	74 - 125	10.0 ± 10.2	26.0 ± 8.2	-0.031	1.73	2.21	27.7
	FR11	76.0	80 - 205	14.0 ± 10.2	25.4 ± 8.3	-0.156	2.16	2.80	29.3
	FR12	41.9	115 - 217	13.9 ± 8.2	25.1 ± 10.2	0.141	3.06	3.03	-0.8

3.2. Turnover dynamics

Canopy turnover was higher in the second interval for both intact and fragmented forest areas (Figure 3). Annualized rates of canopy turnover within the intact forest segments of ST1 increased from 1.68 - 1.95% yr^{-1} (mean of 1.81% yr^{-1}) in the t1-t2 interval to 2.51 - 3.13% yr^{-1} (mean of 2.85% yr^{-1}) in the t2-t3 interval. The range of annualized turnover during each interval was larger for forest fragments of ST2, but turnover rates also increased between the first time interval (1.36 - 3.06% yr^{-1}, mean of 1.98% yr^{-1}) and the second time interval (2.17 - 4.70% yr^{-1}, mean of 3.12% yr^{-1}). The magnitude of change in turnover rates was consistent across the five ST1 segments of intact forest. Meanwhile, there was more variation observed in the magnitude of change in turnover rates among the ST2 forest fragments: turnover more than doubled in FR01 and FR02, nearly doubled in FR03 and FR05, while FR09 showed only a slight increase over time and the turnover rate in FR12 was slightly (0.8%) lower in the second interval (Table 1).

The average number of turnover events also increased between time periods, going from 6.5 to 10.2 events ha^{-1} yr^{-1} (intact forest) and from 7.6 to 10.9 events ha^{-1} yr^{-1} (fragmented forest). The average size of turnover events stayed relatively constant in the intact forest segments (27.9m^2 in t1-t2 versus 28.0m^2 in t2-t3) and increased slightly in the forest fragments (from 26.6m^2 in t1-t2 to 28.7m^2 in t2-t3). Canopy turnover events were classified into different categories based on size (Figure 4). On average across both forest types, ~75% of turnover events were small (< 25 m^2), ~20% were intermediate (25 - 100 m^2), and ~5% were large (> 100 m^2). Large turnover events accounted for about 40% of the total turnover area, in comparison to the total area in intermediate (32%) and small (28%) turnover events. Differences in the observed proportions between time intervals were small (< 2.7%). Examining all study areas, no clear pattern emerged in the size distribution of smaller turnover events between 2013-2014 and 2014-2016.

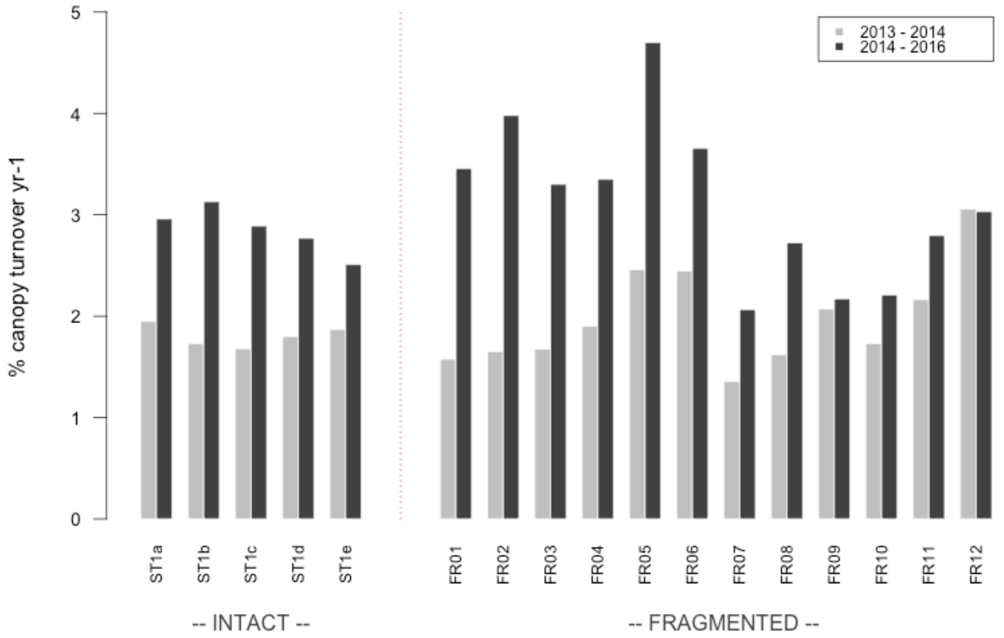

Figure 3. Annualized rates of canopy turnover in intact and fragmented forest areas for the time periods 2013-14 (light gray) and 2014-16 (dark gray).

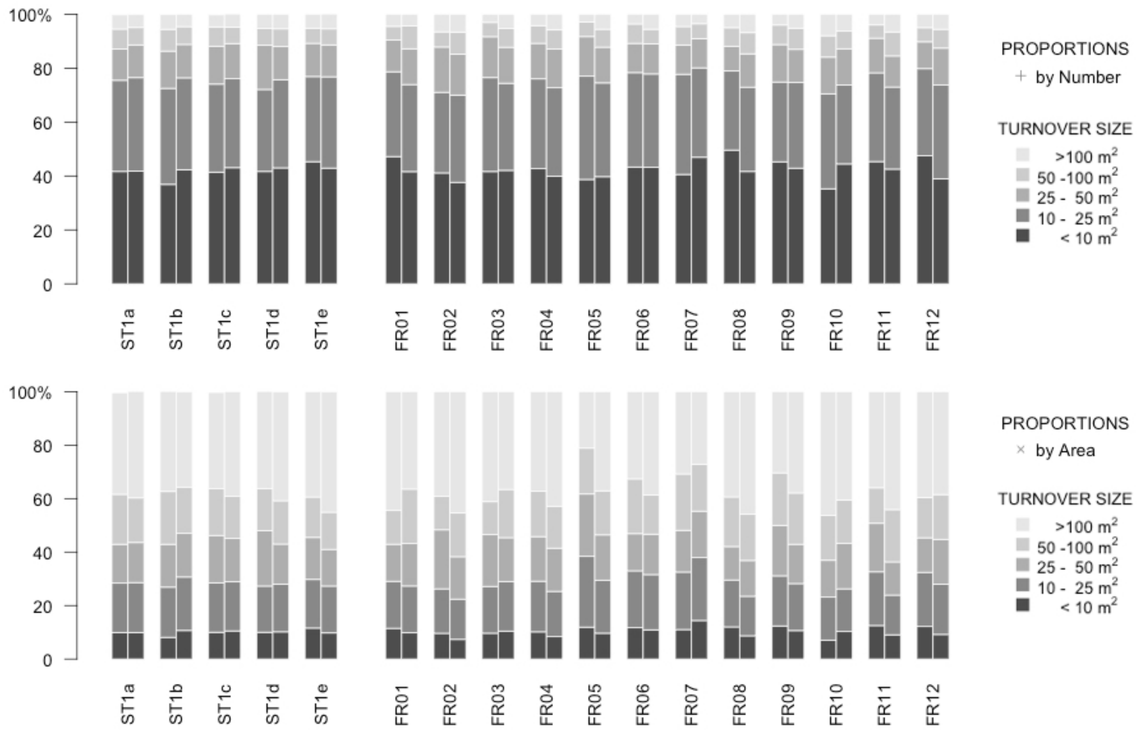

Figure 4. Stacked bar plots show the proportion of canopy turnover event counts (upper panel) and total turnover area (lower panel) by size class in intact (ST1a-e) and fragmented (FR01-12) forest areas.

4. Conclusions

Our study compared canopy turnover dynamics in intact and fragmented forests of the Tapajós National Forest region, including evidence for interannual variability in canopy turnover. Estimated turnover rates were higher in forest fragments than in intact forests in both time periods examined. The fraction of estimated turnover area in small, intermediate and large size classes was consistent across intact forest areas. The same overall pattern was observed in fragmented forests, although there was more variation in the relative proportions of turnover area in different size classes among forest fragments. Canopy turnover was higher during the second time interval (2014-16) that covered a strong El Niño drought in 2015-2016. Our study suggests that drought conditions may have increased the rates of canopy turnover across all forests, as the increase in turnover was nearly equivalent across intact (58.6%) and fragmented (62.7%) forest types. Increased turnover during the 2014-2016 interval was from all size classes. Previous studies have suggested that large trees may be more susceptible to drought-induced mortality (e.g., Nepstad et al., 2007). We observed an overall increase in the number of large turnover events, but the proportion of turnover in different size classes was preserved. Given the two-year sampling interval, it is not possible to specifically attribute the higher turnover to drought conditions, as changes in convective activity or other factors may have increased windthrow before or after the most intense drought effects. Regardless, evidence for large interannual variability in canopy turnover in Amazon forests suggests that forest dynamics may strongly influence regional carbon cycling. Such changes are unlikely to be captured by existing inventory plot networks or moderate resolution satellite data. Airborne lidar provides an efficient means to characterize short-term changes in Amazon forest dynamics over large areas needed to estimate the spatial and temporal variability in canopy turnover.

Acknowledgements

This research was supported by NASA's Terrestrial Ecology and Carbon Monitoring System Programs and Brazilian National Council for Scientific and Technological Development (CNPq, grant 457927/2013-5) and Ciência sem Fronteiras Program (award to D. Morton). Lidar data were acquired with support from USAID, the US Department of State, EMBRAPA and the US Forest Service Office of International Programs.

References

Asner, G. P.; Kellner, J. R.; Kennedy-Bowdoin, T.; Knapp, D. E.; Anderson, C.; Martin, R. E. Forest Canopy Gap Distributions in the Southern Peruvian Amazon. **PLoS ONE**, v. 8, e60875, 2013.

Brienen, R. J. W.; Phillips, O. L.; Feldpausch, T. R.; Gloor, E.; Baker, T. R.; Lloyd, J.; Lopez-Gonzalez, G.; et al. Long-term decline of the Amazon carbon sink. **Nature**, 519, p. 344-348, 2015.

Chambers, J. Q.; Negron-Juarez, R. I.; Marra, D. M.; Di Vittorio, A.; Tews, J., et al. The steady-state mosaic of disturbance and succession across an old-growth Central Amazon forest landscape. **PNAS**, 110(10), p. 3949 - 3954, 2013.

Cook, B. D.; Corp, L. A.; Nelson, R. F.; Middleton, E. M.; Morton, D. C.; McCorkel, J. T.; Masek, J. G.; et al. NASA Goddard's LiDAR, Hyperspectral and Thermal (G-LiHT) Airborne Imager. **Remote Sensing**, 5(8), p. 4045-4066, 2013.

Espírito-Santo, F. D. B.; Gloor, M.; Keller, M.; et al. Size and frequency of natural forest disturbances and the Amazon forest carbon balance. **Nature Communications**, 5:4434, 2014.

Feldpausch, T. R.; Phillips, O. L.; Brienen, R. J. W.; Gloor, E.; Lloyd, J.; Lopez-Gonzalez, G.; et al. Amazon forest response to repeated droughts. **Global Biogeochemical Cycles**, 30, p. 964-982, 2016.

Gatti, L. V.; Gloor, M.; Miller, J. B.; Doughty, C. E.; Malhi, Y.; Domingues, L. G.; et al. Drought sensitivity of Amazonian carbon balance revealed by atmospheric measurements, **Nature**, v. 506, n.7486, p. 76–80, 2014.

Hansen, M. C.; Potapov, P. V.; Moore, R.; Hancher, M.; Turubanova, S. A.; Tyukavina, A.; Thau, D.; et al. High-Resolution Global Maps of 21st-Century Forest Cover Change. **Science**, 342, p. 850, 2013.

Hunter, M. O.; Keller, M.; Morton, D.C.; Cook, B. D.; Lefsky, M.; Ducey, M.; et al. Structural Dynamics of Tropical Moist Forest Gaps. **PLoS ONE**, 10(7): e0132144, 2015.

Le Quéré, C.; Andrew, R. M.; Canadell, J. G.; Sitch, S.; Korsbakken, J. I.; Peters, G. P.; Manning, A. C.; et al. Global Carbon Budget 2016, **Earth System Science Data**, 8, p. 605-649, 2016.

Lloyd, J.; Gloor, E. U. and Lewis, S. L. Are the dynamics of tropical forests dominated by large and rare disturbance events? **Ecology Letters**, 12, E19–E21, 2009.

Longo, M.; Keller, M. M.; dos-Santos, M. N.; Leitold, V.; Pinagé, E. R.; et al. Aboveground biomass variability across intact and degraded forests in the Brazilian Amazon. **Global Biogeochemical Cycles**, 30, doi: 10.1002/2016GB005465, 2016.

Marvin, D. C. and Asner, G. P. Branchfall dominates annual carbon flux across lowland Amazonian forests. **Environmental Research Letters**, 11, 094027, 2016.

Nepstad, D. C.; Tohver, I. M.; Ray, D.; Moutinho, P.; and Cardinot, G. Mortality of large trees and lianas following experimental drought in an Amazon forest. **Ecology**, 88(9), p. 2259-2269, 2007.

Pan, Y.; Birdsey, R. A.; Fang, J.; Houghton, R.; Kauppi, P. E.; Kurz, W. A.; Phillips, O. L.; et al. A Large and Persistent Carbon Sink in the World's Forests. **Science**, 333, p. 988-993, 2011.

Phillips, O. L.; Aragão, L. E. O. C.; Lewis, S. L.; Fisher, J. B.; Lloyd, J.; López-González, G.; Malhi, Y.; et al. Drought Sensitivity of the Amazon Rainforest. **Science**, 323, p. 1344-1347, 2009.

Sustainable Landscapes Brazil Project. Available at: https://www.paisagenslidar.cnptia.embrapa.br/webgis/ Accessed on: Nov. 1., 2016.

USGS Earth Explorer. Available at: http://earthexplorer.usgs.gov/ Accessed on: Nov. 1., 2016.

van der Werf, G. R. et al. Global fire emissions and the contribution of deforestation, savanna, forest, agricultural, and peat fires (1997-2009). **Atmospheric Chemistry and Physics**, 10, p. 11707-11735, 2010.